Mathematical Modeling of the Phase Behaviors of Solid-Polymer-Electrolyte/Salt Systems in Lithium Secondary Batteries: The Nonrandomness Effect

Sung Jin Pai,[1] Young Chan Bae,[1] Sung Ho Kong,[2] Si Ok Ryu[3]

[1]*Division of Chemical Engineering and Molecular Thermodynamics Laboratory, Hanyang University, Seoul 133-791, Korea*

[2]*Department of Chemical Engineering and Environmental Chemical Engineering Lab., Hanyang University, Seoul 133-791, Korea*

[3]*National Research Laboratory, School of Chemical Engineering and Technology, Yeungnam University, Gyoungsan 712-749, Korea*

Received 17 December 2003; accepted 5 April 2004
DOI 10.1002/app.20866
Published online in Wiley InterScience (www.interscience.wiley.com).

ABSTRACT: We establish a new melting-point-depression theory, based on the modified-double-lattice model, that takes into account the local composition concept to describe the phase behaviors of solid-polymer-electrolyte/salt systems (modified-double-lattice/nonrandom model). In comparison with experimental data, quantitative descriptions of the proposed model show better agreement for the given systems than those of the modified-double-lattice model. The systems studied in this work are combinations of poly(ethylene oxide) and zinc halides and of poly(ethylene oxide) and $LiCF_3SO_3$. The results show that the nonrandomness effect of the salt distribution plays a major role in determining the eutectic points of the given systems. © 2004 Wiley Periodicals, Inc. J Appl Polym Sci 94: 231–237, 2004

Key words: conducting polymers; lattice models; melting point; modeling; phase diagrams

INTRODUCTION

Lithium-ion polymer batteries are based on lithium, the lightest metal with the highest electrochemical potential of any solid. However, pure lithium by itself is unstable, so carbon is used as the anode, and the lithium ion can be intercalated. Currently, there are two different types of lithium-ion batteries, and this causes some confusion in the industry. The first type of lithium-ion battery uses a liquid electrolyte and has been on the market for a few years. The second type, a lithium-ion polymer battery, uses a solid polymer electrolyte (SPE) and is currently making an impact in the marketplace. An SPE in a lithium-ion polymer battery acts as both a separator and an electrolyte, providing greater flexibility and safety than a liquid electrolyte.[1]

Since the concept of SPEs was first proposed by Wright,[2] global interest has especially been focused on polymer electrolyte batteries because of their high energy density, safety, and flexibility in fabrication.

Highly conducting polymer electrolytes have been developed for use in reliable electrochemical devices, and much research on SPEs has been performed by many research groups, such as those of Armand,[3] Archer and Armstrong,[4] and Papke.[5] This research has been directed toward the development of SPEs with high ionic conductivity at the ambient temperature. For increased ionic conductivity of SPEs, a polymer should have a low glass-transition temperature and low crystallinity. Reibel et al.[6] described the ionic conductivity of poly(ethylene oxide) (PEO)/lithium bis(4-nitrophenylsulfonyl)imide and PEO/lithium bis(trifluoromethane sulfonyl)imide systems used as polymer electrolytes. Sreekanth et al.[7] reported an application of PEO complexed with $NaNO_3$ salt as an electrochemical cell. Andreev and Bruce[8] reported the structure–conductivity relationship of PEO/$LiAsF_6$ in an analogous phase. Reddy and Chu[9] also reported the structure–conductivity relationship of PEO solvated by a potassium ionic salt.

Smith and Pennings[10] showed that, according to Flory's melting-point-depression theory, a eutectic point may occur in an athermal polymer/diluent system if the melting temperature (T_m) of the diluent is

Correspondence to: Y. C. Bae (ycbae@hanyang.ac.kr).
Contract grant sponsor: Ministry of Information and Communication of Korea (through the Support Project of the University Information Technology Research Center supervised by IITA).

not too low in comparison with that of the polymer. For example, Gryte et al.[11] reported crystallization characteristics of a PEO/glutaric acid system, and Myasnikova et al.[12] provided a phase diagram of a PEO/resorcinol system in which the resorcinol molecules formed hydrogen bonds with the polymer chain.

Recently, Bae's group[13–15] investigated this subject with various thermodynamic theories describing the phase behaviors of SPE/salt systems. These theories can describe various effects (e.g., pressure and free-volume effects) and agree with experimental data remarkably well, but some deviations still exist. The disadvantage of SPEs is the ionic conductivity, which accounts for how well lithium cations are transported in electrolytes. In a real electrolyte system, salts are not distributed randomly, so cations are well transported in some parts and poorly transported in other parts. This phenomenon affects the ionic conductivity of SPEs, so it is necessary to consider the contribution of the nonrandomness effect in a theoretical model.

To describe the nonrandomness effect, the theories include a local composition concept in terms of the interaction energy based on the expressions proposed by Wilson.[16] However, these theories have been seriously questioned by Flemr[17] and McDermott and Ashton.[18] Flemr showed that these equations are inconsistent with the nonrandom assumption from which they are derived because the expressions of Wilson depend only on the interaction energy and not on the composition. Trying to overcome this limitation, Panayiotou and Vera[19] developed a nonrandom-factor (NRF) model that takes into account the dependence of the local composition on the concentration.

The purpose of this work is to establish a new melting-point-depression theory, based on the modified-double-lattice (MDL) model,[20] that takes into account the local composition concept to describe the phase behaviors of SPE/salt systems [the modified-double-lattice/nonrandom (MDL/NR) model]. We used the NRF proposed by Panayiotou and Vera[19] to examine the local composition in SPE/salt systems. We then extend it to the melting-point-depression theory to evaluate T_m of the given systems. A theoretical T_m prediction is compared with experimental data for PEO/zinc halide and PEO/$LiCF_3SO_3$ systems, which are model systems showing changes in the liquid curve and a eutectic point with various salt compositions.

MODEL DESCRIPTION

In this work, we develop a new thermodynamic framework to describe the nonrandom distribution of salt in SPE systems. Three theoretical aspects are taken into account:

1. The MDL model to express a specific interaction.
2. The NRF model to consider the nonrandom distribution of salt (the MDL/NR model).
3. Flory's melting-point-depression theory[21] to correlate the chemical potential to the experimental T_m data.

The chemical potential is calculated as a sum of two contributions:

$$\left(\frac{\mu}{kT}\right) = \left(\frac{\mu}{kT}\right)_{\mathrm{MDL}} + \left(\frac{\mu}{\mathrm{kT}}\right)_{\mathrm{NR}} \quad (1)$$

where k is Boltzmann's constant and T is the temperature. We assume that the salt is a particle to consider a salt effect of the free energy of mixing.

MDL model

Hu and coworkers[22,23] developed an expression for the Helmholtz energy of mixing for binary polymer solutions with the double-lattice model (DLM). Oh and Bae[20] modified the DLM by introducing a new interaction parameter and simplifying the expression.

At temperature T, the canonical partition function of the primary lattice for a binary mixture (Q) is given by

$$Q = \sum_{N_{12}} g(N_1,r_1,N_2,r_2,N_{12}) \times \left[\exp\left(\frac{\varepsilon_{11}}{kT}\right)\right]^{N_{11}}\left[\exp\left(\frac{\varepsilon_{22}}{kT}\right)\right]^{N_{22}}\left[\exp\left(\frac{\varepsilon_{12}}{kT}\right)\right]^{N_{12}} \quad (2)$$

where N_1 and N_2 are the numbers of molecules of the solvent and polymer, respectively. N_{11}, N_{22}, and N_{12} are the numbers of 1–1, 2–2, and 1–2 nearest neighbor (nonbonded) segment–segment pairs, respectively. r_2 is the number of segments in the polymer molecule with respect to $r_1 = 1$ for the solvent. $g(N_1,r_1,N_2,r_2,N_{12})$ is a combinatorial factor that depends on the number of 1–2 segment–segment pairs. The positive energy parameters, ϵ_{11}, ϵ_{22}, and ϵ_{12}, are related to the corresponding nearest neighbor segment–segment interactions.

Primary lattice

The general form of the Helmholtz energy of mixing, based on Freed's theory,[24–26] can be expressed as follows:

$$\frac{\Delta A}{N_r kT} = (\phi_1/r_1)\ln\phi_1 + (\phi_2/r_2)\ln\phi_2 + \sum_m\sum_n \alpha_{mn}\phi_1^m\phi_2^n \quad (3)$$

where ΔA is the Helmholtz energy of mixing, N_r is the number of lattice sites for the mixture, and ϕ_i is the volume fraction of component i. a_{am} is a function of the

coordination number (z), r_1 and r_2, and energy parameters. To obtain an analytically simple expression for the Helmholtz energy of mixing for the primary lattice, Oh and Bae[20] modified Hu et al.'s[22] expressions for a_{mn} in the form of the Flory–Huggins theory. This expression is

$$\frac{\Delta A}{N_r kT} = (\phi_1/r_1)\ln\phi_1 + (\phi_2/r_2)\ln\phi_2 + \chi_{OB}\phi_1\phi_2 \quad (4)$$

where &kggr;$_{OB}$ is defined by

$$\chi_{OB} = C_\beta\left(\frac{1}{r_2} - \frac{1}{r_1}\right)^2 + 2\left(\frac{1}{r_2} - \frac{1}{r_1}\right)\tilde{\varepsilon} - \left(\frac{1}{r_2} - \frac{1}{r_1} + C_\gamma\tilde{\varepsilon}\right)\tilde{\varepsilon}\phi_2 + C_\gamma\tilde{\varepsilon}^2\phi_2^2 \quad (5)$$

where C_β and C_γ are universal constants (0.1415 and 1.7986, respectively). These parameters are obtained through fitting to the simulation data.[20] $\tilde{\varepsilon}$ is a reduced interaction parameter:

$$\tilde{\varepsilon} = \frac{\varepsilon}{kT} = \frac{(\varepsilon_{11} + \varepsilon_{22} - 2\varepsilon_{12})}{kT} \quad (6)$$

Secondary lattice

In Freed's theory, the solution of the Helmholtz energy of mixing for the Ising model is

$$\frac{\Delta A}{N_r kT} = x_1\ln x_1 + x_2\ln x_2 + \frac{z\tilde{\varepsilon}x_1x_2}{2} - \frac{z\tilde{\varepsilon}^2x_1^2x_2^2}{4} + \ldots \quad (7)$$

where x_i is the molar fraction of component i.

To obtain an analytical expression for the secondary lattice, Hu et al.[22] revised eq. (7) to improve the coexistence curves by introducing two empirical coefficients and adding the additional energy of the reference state. Oh and Bae[20] corrected a new Helmholtz energy of mixing as a fractional form to improve the mathematical approximation defect and to reduce the number of parameters:

$$\frac{\Delta A_{sec,ij}}{N_{ij}kT} = \frac{2}{z}\left[\eta\ln\eta + (1-\eta)\ln(1-\eta) + \frac{zC_\alpha\delta\tilde{\varepsilon}_{ij}(1-\eta)\eta}{1 + C_\alpha\delta\tilde{\varepsilon}_{ij}(1-\eta)\eta}\right] \quad (8)$$

where $\Delta A_{sec,ij}$ is the Helmholtz energy of mixing of the secondary lattice for an i–j segment–segment pair and N_{ij} is the number of i–j pairs. $\delta\ \tilde{\varepsilon}_{ij}$ is the reduced energy parameter contributed by the oriented interactions, η is the surface fraction permitting oriented interactions, and C_α is a universal constant (0.4881).

Incorporation of the secondary lattice into the primary lattice

To account for the oriented interaction, a secondary lattice is used. The secondary lattice contribution is a perturbation of the primary lattice. To incorporate a secondary lattice, ϵ_{ij} is replaced by $\epsilon_{ij} - \Delta A_{sec,ij}/N_{ij}$ in eq. (2). According to the definition of ϵ in eq. (6), if oriented interactions occur in i–j segment–segment pairs, $\tilde{\varepsilon}$ is replaced by

$$\frac{\varepsilon}{kT} - \left[\sum_i\left(\frac{\Delta A_{sec,ii}}{N_{ii}kT}\right) - 2\left(\frac{\Delta A_{sec,ij}}{N_{ij}kT}\right)\right] \quad (9)$$

Correlating equations

To correlate the MDL model with the melting-point-depression theory, we require the chemical potentials of components 1 and 2. The definition of the chemical potential is

$$\frac{\Delta\mu_i}{kT} = \frac{\partial(\Delta A/kT)}{\partial N_i} \quad (10)$$

The final expression for the chemical potential can be written as follows:

$$\frac{\Delta\mu_1}{kT} = \ln(1-\phi_2) - r_1\left(\frac{1}{r_2} - \frac{1}{r_1}\right)\phi_2 + r_1\left\{C_\beta\left(\frac{1}{r_2} - \frac{1}{r_1}\right)^2 + \left[\left(\frac{1}{r_2} - \frac{1}{r_1}\right) + C_\gamma\tilde{\varepsilon}\right]\tilde{\varepsilon} + \left(2 + \frac{1}{r_2}\right)\tilde{\varepsilon}\right\}\phi_2^2 - 2r_1\left\{\left[\left(\frac{1}{r_2} - \frac{1}{r_1}\right) + C_\gamma\tilde{\varepsilon}\right]\tilde{\varepsilon} + C_\gamma\tilde{\varepsilon}^2\right\}\phi_2^3 + 3r_1C_\gamma\tilde{\varepsilon}^2\phi_2^4 \quad (11)$$

$$\frac{\Delta\mu_2}{kT} = \ln\phi_2 + r_2\left[\left(\frac{1}{r_2} - \frac{1}{r_1}\right) + C_\beta\left(\frac{1}{r_2} - \frac{1}{r_1}\right)^2 + \left(2 + \frac{1}{r_2}\right)\tilde{\varepsilon}\right] - r_2\left\{\left(\frac{1}{r_2} - \frac{1}{r_1}\right) + 2\left[\left(\frac{1}{r_2} - \frac{1}{r_1}\right) + C_\gamma\tilde{\varepsilon}\right]\tilde{\varepsilon} + 2C_\beta\left(\frac{1}{r_2} - \frac{1}{r_1}\right)^2 + 2\left(2 + \frac{1}{r_2}\right)\tilde{\varepsilon}\right\}\phi_2 + r_2\left\{4\left[\left(\frac{1}{r_2} - \frac{1}{r_1}\right) + C_\gamma\tilde{\varepsilon}\right]\tilde{\varepsilon} + \left(2 + \frac{1}{r_2}\right)\tilde{\varepsilon} + C_\beta\left(\frac{1}{r_2} - \frac{1}{r_1}\right)^2 + 3C_\gamma\tilde{\varepsilon}^2\right\}\phi_2^2 - r_2\left\{6C_\gamma\tilde{\varepsilon}^2 + 2\left[\left(\frac{1}{r_2} - \frac{1}{r_1}\right) + C_\gamma\tilde{\varepsilon}\right]\tilde{\varepsilon}\right\}\phi_2^3 + 3r_2C_\gamma\tilde{\varepsilon}^2\phi_2^4 \quad (12)$$

where ϕ_i is the segment fraction of component i ($\phi_i = N_i r_i / N_r$), and $N_r = \sum_i^m N_i r_i$ is the total number of segments in the system, and r_i is the segment number for component 1 (salt) or 2 (polymer).

Quasichemical approach to the nonrandomness effect

Evaluation of the NRF

For the local composition contribution, we use the NRF model of Panayiotou and Vera.[19] In the NRF model, expressions for local compositions are directly obtained when the surface areas of all the molecules are considered to be the same. In general, the local surface area fractions are related to the overall area fractions:

$$\theta_{ji} = \theta_j \Gamma_{ji} \tag{13}$$

This is the local surface fraction of component j available for contact with component i. θ_j is the overall surface area fraction of component j:

$$\theta_j \equiv \frac{N_j z q_j}{N z q} \tag{14}$$

with $Nzq = \sum_m N_m z q_m$, where N_i is the number of molecules and q_i is a parameter proportional to the molecule's external surface area of component i. zq_i is the surface area parameter:

$$zq_i = r_i(z - 2) + 2 \tag{15}$$

The NRF has to meet the symmetry condition:

$$\Gamma_{ji} = \Gamma_{ij} \ (i \neq j) \tag{16}$$

The correlation of the NRF between i–j pairs is given by

$$\Gamma_{ii}\Gamma_{jj} = G_{ij}\Gamma_{ij}^2 \tag{17}$$

where

$$G_{ij} \equiv \exp(\alpha \Delta\delta\tilde{\varepsilon})(\Delta\delta\tilde{\varepsilon} = \delta\tilde{\varepsilon}_{11} + \delta\tilde{\varepsilon}_{22} - 2\delta\tilde{\varepsilon}_{12}) \tag{18}$$

In eq. (18), α is introduced to represent the degree of nonrandomness, which has previously been presented in the NRTL equation.[27] An additional correlation to define the NRF is given by

$$\Gamma_{ii} = \frac{1 - \sum_{j \neq i} \theta_i \Gamma_{ij}}{\theta_i} \tag{19}$$

where all the $\Gamma_{ij} (i \neq j)$'s are considered to be independent variables.

For binary systems, the solution to eqs. (17) and (19) was given by Guggenheim.[28] Combining the three equations arising in this case from eqs. (17) and (19), we can obtain the NRF as follows:

$$\Gamma_{12} = \frac{2}{1 + [1 - 4\theta_1\theta_2(1 - G_{12})]^{1/2}} \tag{20}$$

Chemical potential of the local composition contribution

Following the work of Panayiotou and Vera,[19] which applies the quasichemical expression for the local surface fractions to different theories of fluids, we can express the excess Helmholtz energy of a polymer solution as the sum of two contributions. One is the random contribution for a polymer solution (A^0), and the other is the local composition contribution (A^{LC}):

$$A = A^0 + A^{LC} \tag{21}$$

We use the modified DLM for the random contribution of the polymer solution and employ Guggenheim's[28] expression for the local composition contribution. Guggenheim derived an expression for the activity of component i in a multicomponent mixture:

$$\ln\gamma_i = (\ln\gamma_i)^0 + \frac{zq_i}{2} \ln\Gamma_{ii} \tag{22}$$

where $(\ln \gamma_i)^0$ is the random contribution to the activity coefficient.

Equation (22) is used for a homogeneous molecule. If the case is nonhomogeneous, the model must consider the unit contribution. From eq. (22), the local composition contribution to the chemical potential is

$$\frac{\Delta\mu_i^{LC}}{kT} = \frac{zq_i}{2} \ln\Gamma_{ii} \tag{23}$$

Here the NRF, Γ_{ii}, is calculated from eqs. (19) and (20).

Melting-point-depression theory

In a semicrystalline system, the condition of equilibrium between a crystalline polymer and a polymer unit in a solution may be described as follows:[21]

$$\mu_u^c - \mu_u^0 = \mu_u - \mu_u^0 \tag{24}$$

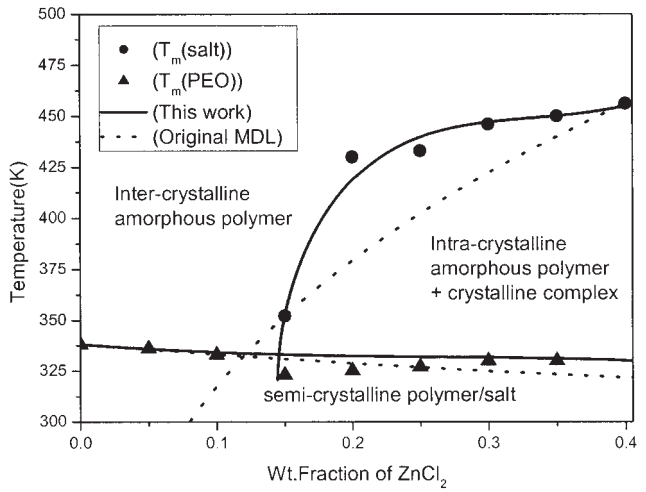

Figure 1 Phase diagram of the PEO/$ZnCl_2$ system. The filled circles and triangles represent the experimental T_m data reported by Kim and Bae.[29] The solid lines represent calculations of the proposed model, and the dashed lines represent calculations of the MDL model.

where μ_u^c, μ_u, and μ_u^0 are the chemical potential of the crystalline polymer segment unit, the chemical potential of the liquid (amorphous) polymer segment unit, and the chemical potential in the standard state, respectively. The formal difference, appearing on the left-hand side, is expected to be as follows:

$$\mu_u^c - \mu_u^0 = -\Delta H_u(1 - T/T_m^0) \tag{25}$$

where ΔH_u is the heat of fusion per segment unit and T and T_m^0 are the melting temperatures of the species in a mixture and in a pure phase, respectively. The right-handed side of eq. (24) can be restated as follows:

$$\mu_u - \mu_u^0 = \frac{V_u}{V_1}\frac{r_1}{r_2}\left(\frac{\partial \Delta A}{\partial N_2}\right)_{T,V,N_1} \tag{26}$$

where V_1 and V_u are the molar volumes of the salt and the repeating unit, respectively. By substituting eqs. (25) and (26) into eq. (24) and replacing T by $T_{m,2}$, we obtain the equilibrium melting temperature of the mixture:

$$\frac{1}{T_{m,2}} - \frac{1}{T_{m,2}^0} = -\frac{k}{\Delta H_u}\frac{V_u}{V_1}\frac{r_1}{r_2}\left(\frac{\mu_2 - \mu_2^0}{kT_{m,2}}\right) \tag{27}$$

The subscripts 1, 2, and u refer to the salt, polymer, and polymer segment unit, respectively. Similarly, we obtain

$$\frac{1}{T_{m,1}} - \frac{1}{T_{m,1}^0} = -\frac{k}{\Delta H_1}\left(\frac{\mu_1 - \mu_1^0}{kT_{m,1}}\right) \tag{28}$$

Correlating eqs. (27) and (28) to this work yields

$$\begin{aligned}\frac{1}{T_{m,2}} - \frac{1}{T_{m,20}^0} = &-\frac{k}{\Delta H_u}\frac{V_u}{V_1}\frac{r_1}{r_2}\Bigg(\ln\phi_2 + r_2\Bigg[\left(\frac{1}{r_2} - \frac{1}{r_1}\right) + C_\beta\left(\frac{1}{r_2} - \frac{1}{r_1}\right)^2 + \left(2 + \frac{1}{r_2}\right)\tilde{\varepsilon}\Bigg] - r_2\Bigg\{\left(\frac{1}{r_2} - \frac{1}{r_1}\right) \\ &+ 2\Bigg[\left(\frac{1}{r_2} - \frac{1}{r_1}\right) + C_\gamma\tilde{\varepsilon}\Bigg]\tilde{\varepsilon} + 2C_\beta\left(\frac{1}{r_2} - \frac{1}{r_1}\right]^2 \\ &+ 2\left(2 + \frac{1}{r_2}\right)\tilde{\varepsilon}\Bigg\}\phi_2 + r_2\Bigg\{4\Bigg[\left(\frac{1}{r_2} - \frac{1}{r_1}\right) + C_\gamma\tilde{\varepsilon}\Bigg]\tilde{\varepsilon} + \left(2 + \frac{1}{r_2}\right)\tilde{\varepsilon} \\ &+ C_\beta\left(\frac{1}{r_2} - \frac{1}{r_1}\right)^2 + 3C_\gamma\tilde{\varepsilon}^2\Bigg\}\phi_2^2 - r_2\Bigg\{6C_\gamma\tilde{\varepsilon}^2 + 2\Bigg[\left(\frac{1}{r_2} - \frac{1}{r_1}\right) \\ &+ C_\gamma\tilde{\varepsilon}\Bigg]\tilde{\varepsilon}\Bigg\}\phi_2^3 + 3r_2C_\gamma\tilde{\varepsilon}^2\phi_2^4 + \frac{zq_2}{2}\ln\Gamma_{22}\Bigg)\end{aligned} \tag{29}$$

and

$$\begin{aligned}\frac{1}{T_{m,1}} - \frac{1}{T_{m,1}^0} = &-\frac{k}{\Delta H_1}\Bigg(\ln(1 - \phi_2) - r_1\left(\frac{1}{r_2} - \frac{1}{r_1}\right)\phi_2 \\ &+ r_1\Bigg\{C_\beta\left(\frac{1}{r_2} - \frac{1}{r_1}\right)^2 + \Bigg[\left(\frac{1}{r_2} - \frac{1}{r_1}\right) + C_\gamma\tilde{\varepsilon}\Bigg]\tilde{\varepsilon} + \left(2 + \frac{1}{r_2}\right)\tilde{\varepsilon}\Bigg\}\phi_2^2 \\ &- 2r_1\Bigg\{\Bigg[\left(\frac{1}{r_2} - \frac{1}{r_1}\right) + C_\gamma\tilde{\varepsilon}\Bigg]\tilde{\varepsilon} + C_\gamma\tilde{\varepsilon}^2\Bigg\}\phi_2^3 \\ &+ 3r_1C_\gamma\tilde{\varepsilon}^2\phi_2^4 + \frac{zq_1}{2}\ln\Gamma_{11}\Bigg\}\end{aligned} \tag{30}$$

RESULTS AND DISCUSSION

Figure 1 shows the phase behavior of a PEO/$ZnCl_2$ system. The filled circles represent experimental data

TABLE I
T_m^0, Heat of Fusion (ΔH) Molecular Weight (MW), Density, and V_u for Each Sample[29]

	T_m^0 (K)	ΔH (J/mol)	MW (g/mol)	Density (g/cm^3)	V_u (cm^3/mol)
PEO	338.15	8,284.32[a]	900,000	1.21	36.60
$ZnCl_2$	556.15	6,011.32	136.28	2.91	46.83
$ZnBr_2$	667.15	10,466.82	225.19	4.20	53.60
ZnI_2	719	16,677.13	319	4.74	67.39
$LiCF_3SO_3$	499.29	10,516.48	156.01	2.69	52.66

[a] 8284.32 J/unit.

TABLE II
Model Parameters for the Given Systems

	ε/k (K)	$\delta\varepsilon_{12}$/k (K)	α
PEO/$ZnCl_2$	−217.956	5,596.447	0.028
PEO/$ZnBr_2$	−197.412	7,037.662	0.036
PEO/ZnI_2	−284.404	10,196.348	0.032
PEO/$LiCF_3SO_3$	−12.477	1,825.082	0.055

for the salt-rich phase, and triangles represent data for the polymer-rich phase reported by Kim and Bae.[29] The solid line is the coexistence curve calculated from the MDL/NR model, and the dotted line is from the original MDL model. The polymer-rich liquid curve has been calculated from eq. (29), and the salt-rich curve has been calculated from eq. (30). Table I provides literature data for PEO/salt systems.[29] We allow the number of the salt segment, r_1, to be equal to 1, and we calculate the number of the polymer units, r_2, with specific volumes v_1 and v_2 for the solvent and polymer, respectively:

$$r_2 = \frac{M_2 \nu_2}{M_1 \nu_1} \tag{31}$$

where M_1 and M_2 are the molecular masses of the salt and polymer, respectively. We set η equal to = 0.3 and z equal to 6, as suggested by Hu et al.[22] These are generally accepted as reasonable values. The model parameters for the given systems are listed in Table II.

As shown in Figure 1, the theoretical prediction of the MDL/NR model (solid lines) not only agrees well with the experimental data but also identifies the eutectic point at the intersection of the two liquid curves at a $ZnCl_2$ weight fraction of approximately 0.14. In this system, α is 0.028. The dotted line (the MDL model), however, shows a slight deviation from the experimental data. These results let us deduce that the NRF introduced in the proposed model allows us to obtain a good representation of the T_m data of the real polymer/salt system.

Figures 2 and 3 present the phase behaviors of PEO/$ZnBr_2$ and PEO/ZnI_2 systems, respectively. The experimental data for the PEO/zinc halide systems show that T_m of the semicrystalline phase gradually decreases, and the curve of the intracrystalline phase steeply increases near the eutectic point and then gradually increases as the weight fraction of the salt increases. The MDL/NR model gives a better description of the experimental data than the MDL model for the given systems, specifically near the eutectic point.

The eutectic point, which usually gives the highest ionic conductivity, plays an important role in the design of lithium secondary batteries. Alternatively, the polymer and salt can simultaneously coexist in the melted state at the eutectic point. The eutectic compositions appear at $ZnBr_2 \approx 0.15$ and $ZnI_2 \approx 0.18$, respectively, and α is near 0.03. The results show that the eutectic point moves toward a higher composition as the size of the salt molecule increases.

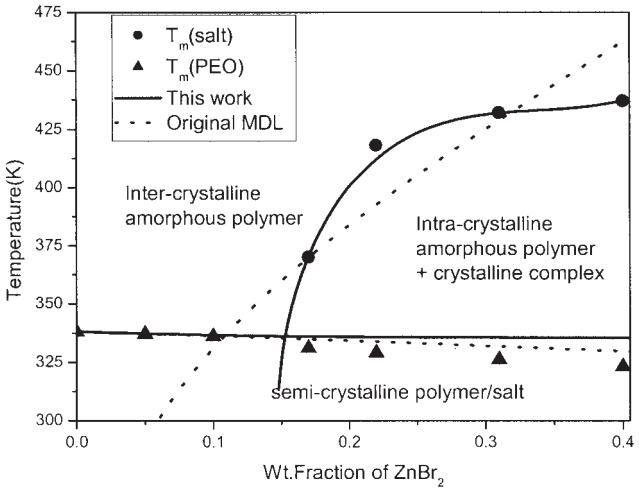

Figure 2 Phase diagram of the PEO/$ZnBr_2$ system. The filled circles and triangles represent the experimental T_m data reported by Kim and Bae.[29] The solid lines represent calculations of the proposed model, and the dashed lines represent calculations of the MDL model.

Figure 4 shows the T_m data for the PEO/$LiCF_3SO_3$ system. The filled circles and triangles represent experimental data reported by Minier et al.[30] This system shows a gradual increase in T_m in the intracrystalline region, but the slope is smaller than that of the PEO/zinc halide system. In this system, there is little deviation from the random model. From this we infer that the components are mixed completely or that the

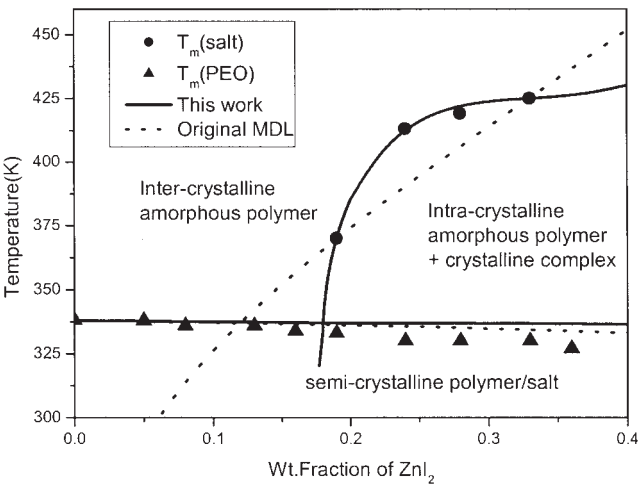

Figure 3 Phase diagram of the PEO/ZnI_2 system. The filled circles and triangles represent the experimental T_m data reported by Kim and Bae.[29] The solid lines represent calculations of the proposed model, and the dashed lines represent calculations of the MDL model.

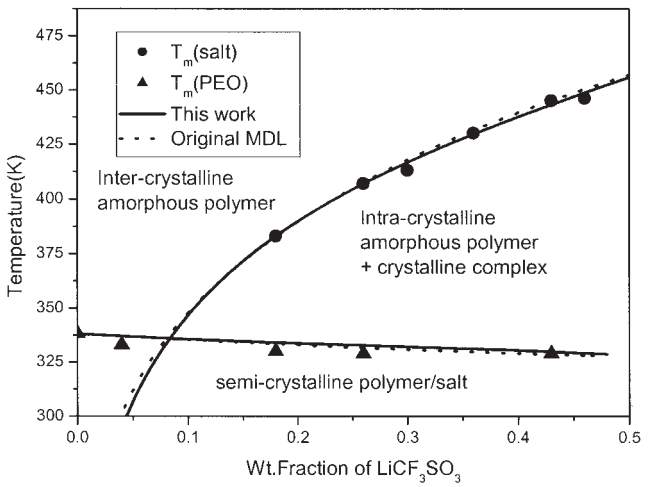

Figure 4 Phase diagram of the PEO/$LiCF_3SO_3$ system. The filled circles and triangles represent the experimental T_m data reported by Minier et al.[30] The solid lines represent calculations of the proposed model, and the dashed lines represent calculations of the MDL model.

interactions between each molecule are similar. The eutectic composition appears at $LiCF_3SO_3 \approx 0.08$ and $\alpha = 0.055$.

CONCLUSIONS

We have established the MDL/NR model, which takes into account the nonrandomness effect in SPEs with a quasichemical approach. The calculated results have been compared with experimental data for SPEs composed of various PEO/salt systems. Good agreement between the theory and experimental data can be obtained when the NRF is introduced. The model can easily be used to evaluate the eutectic points of the given systems.

References

1. Hooper, A.; Ganthier, M.; Bélanger, A. Electrochemical Science and Technology of Polymers; Elsevier Applied Science: London, 1988; Vol. 2.
2. Wright, P. V. Br Polym J 1975, 7, 319.
3. Armand, M. B.; Chabagno, J. M.; Duclot, M. J. Fast Ion Transport in Solids; North Holland: Amsterdam, 1979; p 131.
4. Archer, W. I.; Armstrong, R. D. Electrochim Acta 1980, 25, 1689.
5. Papke, B. L.; Dupon, R.; Rather, M. A.; Shriver, D. F. Solid State Ionics 1981, 5, 685.
6. Reibel, L.; Bayoudh, S.; Baudry, P.; Matstre, H. Electrochim Acta 1998, 43, 1171.
7. Sreekanth, T.; Reddy, M. J.; Ramalingaiah, S.; Subba Rao, U. V. J Power Sources 1999, 79, 105.
8. Andreev, Y. G.; Bruce, P. G. Electrochim Acta 2000, 45, 1417.
9. Reddy, M. J.; Chu, P. P. Electrochim Acta 2002, 47, 1189.
10. Smith, P.; Pennings, A. J. J Polym Sci 1977, 15, 523.
11. Gryte, C. C.; Berghmans, H.; Smets, G. J Polym Sci 1979, 17, 1295.
12. Myasnikova, R. M.; Titova, E. F.; Obolonkova, E. S. Polymer 1980, 21, 403.
13. Kim, J. Y.; Noh, S. T.; Bae, Y. C. Polymer 1998, 39, 3473.
14. Ahn, W. Y.; Bae, Y. C. Electrochim Acta 2000, 45, 3157.
15. Choi, Y. S.; Bae, Y. C. Solid State Ionics 2003, 158, 243.
16. Wilson, G. M. J Am Chem Soc 1964, 86, 127.
17. Flemr, V. Collect Czech Chem Commun 1976, 41, 3347.
18. McDermott, C.; Ashton, N. Fluid Phase Equilib 1977, 1, 33.
19. Panayiotou, C.; Vera, J. H. Fluid Phase Equilib 1980, 5, 55.
20. Oh, J. S.; Bae, Y. C. Polymer 1998, 39, 1149.
21. Flory, P. J. Principles of Polymer Chemistry, 8th ed.; Cornell University Press: Ithaca, New York, 1971; p 568.
22. Hu, Y.; Lambert, S. M.; Soane, D. S.; Prausnitz, J. M. Macromolecules 1991, 24, 4356.
23. Hu, Y.; Lin, H.; Soane, D. S.; Prausnitz, J. M. Fluid Phase Equilib 1991, 67, 65.
24. Freed, K. F. J Phys A: Math Gen 1985, 18, 871.
25. Bawendi, M. G.; Freed, K. F.; Mohanty, U. J Chem Phys 1987, 87, 5534.
26. Bawendi, M. G.; Freed, K. F. J Chem Phys 1988, 88, 2741.
27. Renon, H.; Prausnitz, J. M. J AIChE 1968, 14, 135.
28. Guggenheim, E. A. Proc R Soc London Ser A 1945, 183, 43.
29. Kim, J. Y.; Bae, Y. C. Polymer 1999, 40, 1979.
30. Minier, M.; Berthier, C.; Gorecki, W. J Phys 1984, 45, 739.